



ELSEVIER

Journal of Alloys and Compounds 228 (1995) 172–176

Journal of  
ALLOYS  
AND COMPOUNDS

# Anisotropic Nd–Fe–Co–Zr–B powders prepared by the HDDR process

M. Jurczyk

CSIRO Division of Applied Physics, PO Box 218, Lindfield, N.S.W. 2070, Australia

Received 2 February 1995

## Abstract

Nd<sub>2</sub>Fe<sub>14</sub>B-type powders, where there has been partial substitution of Fe by Zr (up to 1 at.%) and by both Zr and Co, have been prepared by the hydrogenation, disproportionation, desorption, recombination (HDDR) process. Materials with good magnetic properties are obtained for Nd-rich compositions. Powders containing at least 0.3 at.% of Zr, e.g. Nd<sub>1.6</sub>Fe<sub>75.7</sub>Zr<sub>0.3</sub>B<sub>x</sub>, are anisotropic with an intrinsic coercivity of 971 kA m<sup>-1</sup>. The addition of Co to the Zr containing alloy results in an increase in the remanence but a decrease in the coercivity. The powders are of potential use in the manufacture of polymer bonded magnets.

*Keywords:* Anisotropic powders; HDDR process; Magnetic properties

## 1. Introduction

At present the most widely used powder for making polymer bonded NdFeB magnets is made by a rapid solidification process (melt spinning), which produces an isotropic material [1]. New preparation techniques such as mechanical alloying [2] and hydrogenation, disproportionation, desorption, recombination (HDDR) [3–5] are possible candidate processes for the commercial production of NdFeB powders, but they are yet to find widespread use. Mechanical alloying, like melt spinning, produces magnetically isotropic material. Hot pressing and die-upsetting of melt spun and mechanically alloyed material has been used to introduce anisotropy and a high intrinsic coercivity [6].

Harris [4] has reviewed the use of hydrogen in the processing of NdFeB-type magnets, particularly the hydrogen decrepitation (HD) process where the cast coarse grained Nd<sub>16</sub>Fe<sub>76</sub>B<sub>8</sub>-type alloy is reduced to a relatively fine powder by exposure to hydrogen at about 100 kPa pressure and at room temperature. Harris comments that the HD process can be used to make an anisotropic powder from the melt spun and die-upset material, but it is a high cost process. In the HDDR process, NdFeB-type alloys are heated in hydrogen to above 650°C, where the Nd<sub>2</sub>Fe<sub>14</sub>B phase

disproportionates into  $\alpha$ -Fe, Nd-hydride and Fe<sub>2</sub>B [4,7]. The disproportionated material can be recombined by heating under vacuum, resulting in a material made up of a matrix of very fine grains [3]. Thus, the HDDR process consists of four main steps: hydrogenation of Nd<sub>2</sub>Fe<sub>14</sub>B at low temperatures, decomposition of Nd<sub>2</sub>Fe<sub>14</sub>BH<sub>x</sub> into Nd-hydride plus  $\alpha$ -Fe plus Fe<sub>2</sub>B, desorption of H<sub>2</sub> gas from Nd-hydride and finally recombination of Nd plus  $\alpha$ -Fe plus Fe<sub>2</sub>B into Nd<sub>2</sub>Fe<sub>14</sub>B.

Recently, Nakayama et al. [8], using the HDDR process, have shown that the partial substitution of Fe by Co in Nd<sub>2</sub>Fe<sub>14</sub>B, and the addition of a small but a critical concentration of elements such as Ga, Zr, Nb, Hf or Ta can be used to produce anisotropic powders. Harris and co-workers [4,9] has also shown that anisotropic powder, with good magnetic properties, can be made from a Co-free alloy with the partial substitution of Fe by Zr. The best bonded magnets based on Nd<sub>16</sub>Fe<sub>75.9</sub>Zr<sub>0.1</sub>B<sub>8</sub> have an energy product  $(BH)_{\max}$  of about 150 kJ m<sup>-3</sup> and an intrinsic coercivity  $JH_c$  of 800 kA m<sup>-1</sup> [9]. The coercivity can be improved further to about 1.0 MA m<sup>-1</sup> by adding 1 at.% Ga [10].

Here, the relationship between the various HDDR processing parameters and the magnetic properties of Nd<sub>2</sub>Fe<sub>14</sub>B-type materials, where there has been partial

substitution of Fe by Zr (up to 1 at.%) and by both Zr and Co, are studied.

## 2. Material processing

Starting alloys  $\text{Nd}_{12.6}\text{Fe}_{81.4}\text{B}_6$ ,  $\text{Nd}_{16}\text{Fe}_{76-x}\text{Zr}_x\text{B}_8$ ,  $\text{Nd}_{12.6}\text{Fe}_{69.3}\text{Co}_{11.6}\text{Zr}_{0.5}\text{B}_6$ ,  $\text{Nd}_{16}\text{Fe}_{70.2}\text{Co}_{5.3}\text{Zr}_{0.5}\text{B}_8$  and  $\text{Nd}_{16}\text{Fe}_{65.2}\text{Co}_{10.3}\text{Zr}_{0.5}\text{B}_8$ , where  $x = 0, 0.1, 0.3, 0.5$  and  $1.0$  (given in at.%) were prepared by arc melting stoichiometric amounts of the constituent elements (purity 99.9 at.% or better) under an atmosphere of argon. Also, an alloy of nominal composition  $\text{Nd}_{12.6}\text{Fe}_{69.3}\text{Co}_{11.6}\text{Zr}_{0.5}\text{B}_6$  was purchased from Rare-Earth Products Ltd. All the alloys were homogenized at  $1050^\circ\text{C}$  for 24 h to minimize the  $\alpha\text{-Fe}$  content, and in the case of alloys with a Nd content of 12.6 at.% to ensure single phase material with the 2:14:1-type structure. The crystallographic structures of the samples were determined by powder X-ray diffraction (XRD) analysis using Cu  $K\alpha$  radiation. Metallographic studies were performed using a scanning electron microscope (SEM) fitted with an energy-dispersive X-ray microanalysis system (EDS).

The HDDR experiments were carried out in a combined hydrogen–vacuum–annealing system. Ingot pieces of an alloy, weighing about 5–10 g, were placed in the sample chamber at room temperature. The chamber was then evacuated to a vacuum of  $10^{-2}$  Pa and then filled with hydrogen to a pressure of 100 kPa. After completion of the room temperature absorption stage the samples were disproportionated at processing temperatures ranging from  $755\text{--}925^\circ\text{C}$ , using the established method of 2 h under hydrogen, 1 h under vacuum and then slowly cooling over 3 h to room temperature [4].

The XRD patterns in Fig. 1 are representative of a typical  $\text{Nd}_{16}\text{Fe}_{76}\text{B}_8$  alloy at various stages of the HDDR process. The hydrogenation and disproportionation reactions were performed at  $850^\circ\text{C}$ , where the alloy disproportionates into Nd-hydride,  $\text{Fe}_2\text{B}$  and  $\alpha\text{-Fe}$  (Fig. 1(b)). The desorption and recombination stages, to obtain the 2:14:1 phase, were carried out by a heat treatment at  $784^\circ\text{C}$  in high vacuum (about  $10^{-3}$  Pa). After the HDDR process, the alloys were crushed in an agate mortar to produce powder with a grain size less than  $106\ \mu\text{m}$ . Samples for measurements of the magnetic properties were made by mixing the powders with epoxy resin in suitable moulds in an applied magnetic field of  $1.6\ \text{MA m}^{-1}$ .

## 3. Magnetic Properties

The magnetic properties were measured using a vibrating sample magnetometer (VSM) (maximum

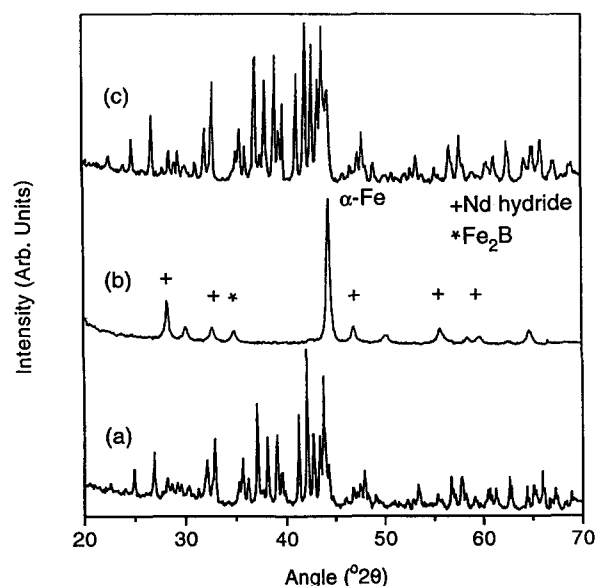


Fig. 1. XRD spectra of  $\text{Nd}_{16}\text{Fe}_{76}\text{B}_8$ : (a) before, (b) after heat treatment at  $850^\circ\text{C}$  in hydrogen for 2 h and (c) after heat treatment in vacuum for 1 h at  $784^\circ\text{C}$ .

field of  $1.6\ \text{MA m}^{-1}$ ) and/or a Quantum Design SQUID magnetometer (maximum field of  $4\ \text{MA m}^{-1}$ ).

Fig. 2 shows the behaviour of the intrinsic coercivity of  $\text{Nd}_{16}\text{Fe}_{76-x}\text{Zr}_x\text{B}_8$ , containing 0.1, 0.3, 0.5 and 1.0 at.% Zr, as a function of the desorption–recombination temperature. A maximum intrinsic coercivity  $J_c$  occurs at a zirconium content of  $x = 0.3$  at.% and its value at room temperature is  $971\ \text{kA m}^{-1}$ , which compares with  $800\ \text{kA m}^{-1}$  reported by McGuiness et al. [9] for  $\text{Nd}_{16}\text{Fe}_{75.9}\text{Zr}_{0.1}\text{B}_8$  material. McGuiness et

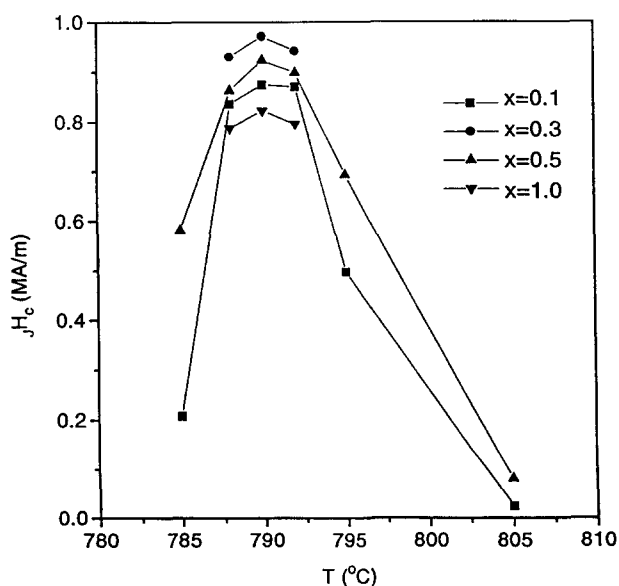


Fig. 2. The variation of the intrinsic coercivity  $J_c$  with desorption–recombination temperature for  $\text{Nd}_{16}\text{Fe}_{76-x}\text{Zr}_x\text{B}_8$  powders ( $x = 0.1, 0.3, 0.5$  and  $1.0$  at.%).

al. noted that the  $\text{Nd}_{16}\text{Fe}_{76-x}\text{Zr}_x\text{B}_8$  alloy containing 0.3 at.% Zr failed to exhibit an intrinsic coercivity greater than  $120 \text{ kA m}^{-1}$ , and the initial fine microstructure had been completely destroyed by large grains [9].

The behaviour of  $J_c$  for  $\text{Nd}_{16}\text{Fe}_{76-x}\text{Zr}_x\text{B}_8$  alloys is similar to that of  $\text{Nd}_{16}\text{Fe}_{76}\text{B}_8$  alloy, where a maximum intrinsic coercivity was observed at the desorption–recombination temperature of  $784^\circ\text{C}$  (see Fig. 3). The  $\text{Nd}_{12.6}\text{Fe}_{81.4}\text{B}_6$  alloy exhibits a narrower maximum at  $798^\circ\text{C}$  with  $J_c$  of  $710 \text{ kA m}^{-1}$  (measured at room temperature). These results are consistent with those reported by McGuinness et al. [9]. Higher  $J_c$  values are obtained in neodymium-rich alloys (see Fig. 3). The maximum in the intrinsic coercivity can be attributed to the establishment of an optimum grain size and the minimization of the  $\alpha\text{-Fe}$  content. SEM examination showed the grain size to be about  $0.5 \mu\text{m}$ , which is close to the single-domain size for the  $\text{Nd}_2\text{Fe}_{14}\text{B}$  phase [11]. Fig. 4 shows the XRD patterns of the  $\text{Nd}_{16}\text{Fe}_{75.5}\text{Zr}_{0.5}\text{B}_8$  material after HDDR processing using three different desorption–recombination temperatures, namely 760, 790 and  $824^\circ\text{C}$ . Processing at a low desorption–recombination temperature results in an unacceptably high content of  $\alpha\text{-Fe}$ . At higher temperatures the intrinsic coercivity is limited by the presence of large grains (equal to or greater than  $5\text{--}10 \mu\text{m}$ ).

The magnetic polarization  $J$  as a function of the applied field  $H$  for the starting  $\text{Nd}_{16}\text{Fe}_{76}\text{B}_8$  powdered material, measured parallel and perpendicular to the directions of alignment, is shown in Fig. 5. Before

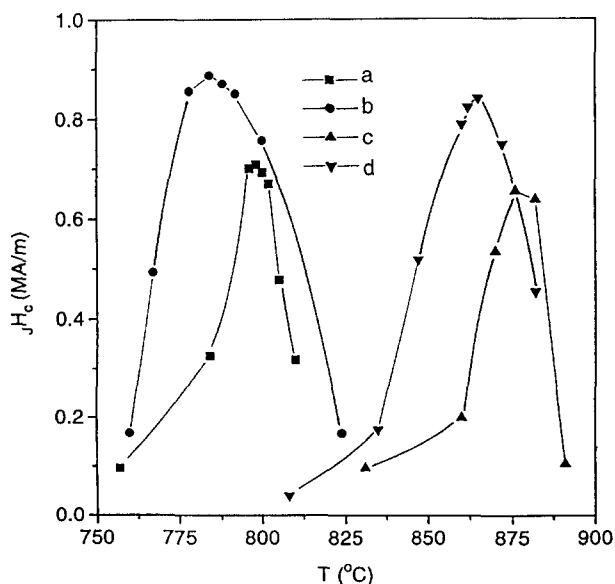


Fig. 3. The variation of the intrinsic coercivity  $J_c$  with desorption–recombination temperature for (a)  $\text{Nd}_{12.6}\text{Fe}_{81.4}\text{B}_6$ , (b)  $\text{Nd}_{16}\text{Fe}_{76}\text{B}_8$ , (c)  $\text{Nd}_{12.6}\text{Fe}_{69.3}\text{Co}_{11.6}\text{Zr}_{0.5}\text{B}_6$  and (d)  $\text{Nd}_{16}\text{Fe}_{65.2}\text{Co}_{10.3}\text{Zr}_{0.5}\text{B}_8$  powders.

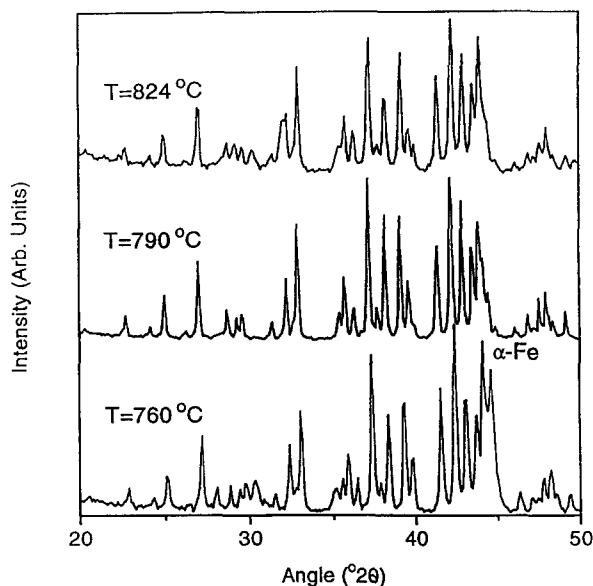


Fig. 4. XRD spectra of  $\text{Nd}_{16}\text{Fe}_{75.5}\text{Zr}_{0.5}\text{B}_8$  after heat treatment at desorption–recombination temperatures of 760, 790 and  $824^\circ\text{C}$  for 1 h.

HDDR treatment the material is anisotropic, but magnetically soft. The HDDR processing produces high intrinsic coercivity but removes any existing anisotropy in  $\text{Nd}_{16}\text{Fe}_{76}\text{B}_8$ . SQUID measurements of the HDDR processed  $\text{Nd}_{16}\text{Fe}_{76-x}\text{Zr}_x\text{B}_8$  ( $0 \leq x \leq 1.0$ ) powders, show evidence of anisotropy for  $x \geq 0.3$  at.% Zr. Three factors, the optimized hydrogenation–disproportionation and desorption–recombination temperatures and Zr content in  $\text{Nd}_2\text{Fe}_{14}\text{B}$ -type materials are essential for producing anisotropic powders. The

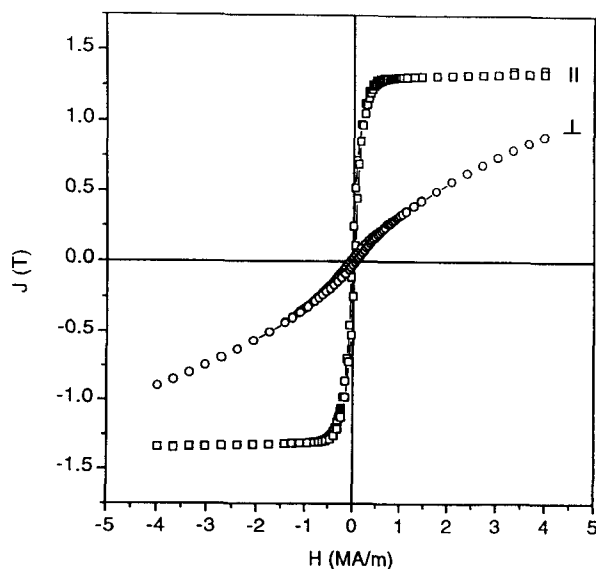


Fig. 5. Magnetic polarization  $J$  as a function of the applied field  $H$  for powders of the starting material  $\text{Nd}_{16}\text{Fe}_{76}\text{B}_8$  measured parallel (||) and perpendicular ( $\perp$ ) to the direction of alignment.

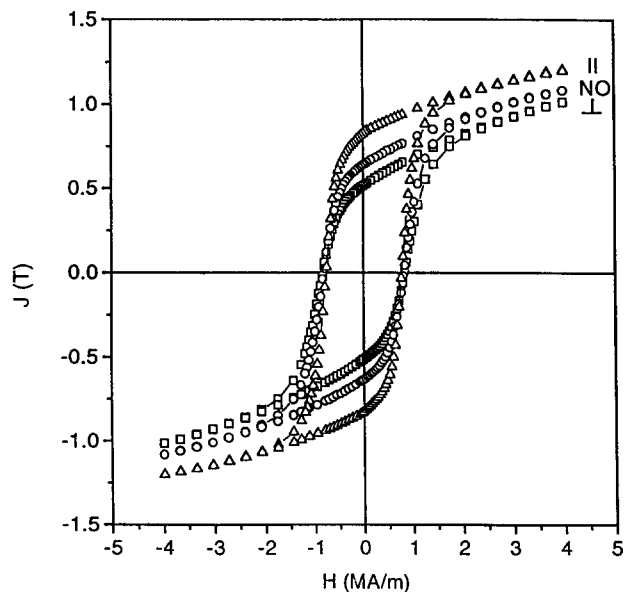


Fig. 6. Magnetic polarization  $J$  as a function of the applied field  $H$  for HDDR-treated  $\text{Nd}_{16}\text{Fe}_{65.2}\text{Co}_{10.3}\text{Zr}_{0.5}\text{B}_8$  powders measured parallel ( $\parallel$ ) and perpendicular ( $\perp$ ) to the direction of alignment (non-oriented (NO) powder is included for reference).

addition of Zr to  $\text{Nd}_2\text{Fe}_{14}\text{B}$ -type material induces anisotropy by decelerating the decomposition of the  $\text{Nd}_2\text{Fe}_{14}\text{B}$  phase, which in turn leads to the formation of nuclei with a preferred orientation [12]. The degree of anisotropy increases for a hydrogenation–disproportionation temperature of about  $100^\circ\text{C}$  higher than the optimum desorption–recombination temperature. Magnetic hysteresis curves for the  $\text{Nd}_{16}\text{Fe}_{65.2}\text{Co}_{10.3}\text{Zr}_{0.5}\text{B}_8$  powder, measured parallel and perpendicular to the aligned directions and for non-oriented material, are shown in Fig. 6. Anisotropic behaviour is clearly evident. The remanent magnetic polarization ratio,  $J_r(\parallel)/J_r(\perp)$ , for  $\text{Nd}_{16}\text{Fe}_{65.2}\text{Co}_{10.3}\text{Zr}_{0.5}\text{B}_8$  powder aligned in a magnetic field (measured parallel to the aligned direction) and for the same powder without alignment, is 1.34, which com-

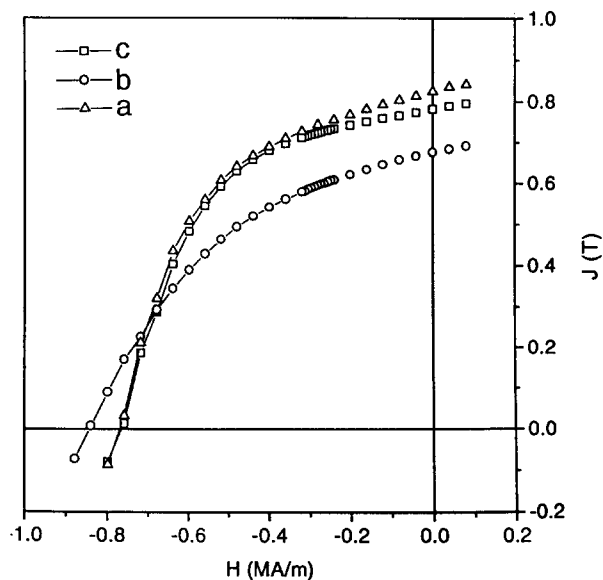


Fig. 7. Demagnetization curves of HDDR-treated (a)  $\text{Nd}_{16}\text{Fe}_{65.2}\text{Co}_{10.3}\text{Zr}_{0.5}\text{B}_8$ , (b)  $\text{Nd}_{16}\text{Fe}_{76}\text{B}_8$  and (c)  $\text{Nd}_{16}\text{Fe}_{75}\text{Zr}_1\text{B}_8$  epoxy bonded powders measured parallel to the direction of alignment (all data has been normalized to 100% density).

pares with a value of 1.42 reported by Nakayama and Takeshita [10] for  $\text{Nd}_{12.6}\text{Fe}_{69.3}\text{Co}_{11.6}\text{Zr}_{0.5}\text{B}_6$  powder (hysteresis loops for aligned and non-aligned powder are not given by Nakayama and Takeshita).

Fig. 7 shows the demagnetization curve for HDDR processed and epoxy bonded  $\text{Nd}_{16}\text{Fe}_{65.2}\text{Co}_{10.3}\text{Zr}_{0.5}\text{B}_8$  powder compared with  $\text{Nd}_{16}\text{Fe}_{76}\text{B}_8$  and  $\text{Nd}_{16}\text{Fe}_{75}\text{Zr}_1\text{B}_8$  powders. The addition of Co to the Zr containing alloy results in an increase in the remanence but a decrease in the coercivity. For materials containing Co and Zr improved squareness of the hysteresis loop is observed. Additionally, Co raises the Curie temperature from 586 K for  $\text{Nd}_{16}\text{Fe}_{76}\text{B}_8$  to 721 K for  $\text{Nd}_{16}\text{Fe}_{65.2}\text{Co}_{10.3}\text{Zr}_{0.5}\text{B}_8$ . Room temperature magnetic properties of the HDDR processed NdFeB-type materials are given in Table 1.

Table 1

Intrinsic coercivity  $JH_c$ , remanent magnetic polarization  $K$ , saturation polarization  $J_s$  at  $4 \text{ MA m}^{-1}$  and  $J_r(\parallel)/J_r(\perp)$  ratio, at room temperature, of HDDR processed and annealed powders measured parallel ( $\parallel$ ) and perpendicular ( $\perp$ ) to the direction of alignment

Material	Direction	$JH_c$ ( $\text{kA m}^{-1}$ )	$J_r$ (T)	$J_s$ (T)	$J_r(\parallel)/J_r(\perp)$
$\text{Nd}_{16}\text{Fe}_{76}\text{B}_8$	$\parallel$	859	0.69	1.11	1.1
	$\perp$	887	0.64	1.11	
$\text{Nd}_{16}\text{Fe}_{75.7}\text{Zr}_{0.3}\text{B}_8$	$\parallel$	971	0.66	1.04	1.2
	$\perp$	971	0.57	1.01	
$\text{Nd}_{16}\text{Fe}_{75}\text{Zr}_1\text{B}_8$	$\parallel$	796	0.77	1.12	1.4
	$\perp$	823	0.57	1.02	
$\text{Nd}_{16}\text{Fe}_{65.2}\text{Co}_{10.3}\text{Zr}_{0.5}\text{B}_8$	$\parallel$	780	0.83	1.20	1.6
	$\perp$	840	0.52	1.03	

#### 4. Conclusions

HDDR processed NdFeB-type powders, with the partial substitution of Fe by Zr (up to 1 at.%) and by both Zr and Co, have been produced. Powders with a Zr content of at least 0.3 at.% are anisotropic with an intrinsic coercivity of  $971 \text{ kA m}^{-1}$ . The degree of anisotropy increases for an hydrogenation–disproportionation temperature about  $100^\circ\text{C}$  higher than the optimum desorption–recombination temperature. The addition of Co to the Zr containing alloy results in improved  $J$ – $H$  loop squareness.

#### Acknowledgment

I thank Dr. S.J. Collocott for useful discussions and C. Andrikidis for assistance with the magnetic measurements. Support for this work was provided by the Australian Department of Industry, Science and Technology under the Generic Technology Component of the Industry Research and Development Act 1986.

#### References

- [1] R.W. Lee, E.G. Brewer and N.A. Schaffel, *IEEE Trans. Magn.*, **21** (1985) 1958.
- [2] L. Schultz, K. Schnitzke and J. Wecker, *J. Appl. Phys.*, **64** (1988) 5302.
- [3] T. Takeshita and R. Nakayama, in *Proc. 10th Int. Workshop on Rare Earth Magnets and their Applications*, Kyoto, Japan, 1989, p. 551.
- [4] I.R. Harris, in *Proc. 12th Int. Workshop on Rare Earth Magnets and their Applications*, Canberra, Australia, 1992, p. 347.
- [5] R. Nakayama, T. Takeshita, M. Itakura, N. Kuwano and K. Oki, *J. Appl. Phys.*, **70** (1991) 3770.
- [6] L. Schultz, K. Schnitzke, J. Wecker, M. Katter and C. Kuhrt, *J. Appl. Phys.*, **70** (1991) 6339.
- [7] P.J. McGuinness, X.J. Zhang, H. Forsyth and I.R. Harris, *J. Less-Common Met.*, **162** (1990) 379.
- [8] R. Nakayama, T. Takeshita, M. Itakura, N. Kuwano and K. Oki, *J. Appl. Phys.*, **76** (1994) 412.
- [9] P.J. McGuinness, C.L. Short and I.R. Harris, *IEEE Trans. Magn.*, **28** (1992) 2160.
- [10] R. Nakayama and T. Takeshita, *J. Alloys Comp.*, **193** (1993) 259.
- [11] J.D. Livingston, *J. Appl. Phys.*, **57** (1985) 4137.
- [12] M. Uehara, H. Tomizawa, S. Hirose, T. Tomida and Y. Maehara, *IEEE Trans. Magn.*, **29** (1993) 2770.